

## ARTICLES

**Spin fluctuations in  $\text{Al}_3\text{V}$ : An NMR study**

Chin-Shan Lue\* and Joseph H. Ross, Jr.†

*Department of Physics, Texas A&M University, College Station, Texas 77843-4242*

(Received 10 August 1998; revised manuscript received 24 May 1999)

We report the results of a nuclear magnetic resonance (NMR) study of  $\text{Al}_3\text{V}$  at temperatures between 4 and 300 K.  $^{51}\text{V}$  and  $^{27}\text{Al}$  Knight shifts exhibit a Curie-Weiss behavior corresponding to an effective moment  $P_{\text{eff}} \approx 0.32\mu_B$  per V, indicating intrinsic weak magnetism localized in vanadium orbitals. The  $T_1$  exhibits a  $\sqrt{T}$  dependence at higher temperatures, indicative of nearly antiferromagnetic behavior of itinerant electrons. We have fit the observed behavior within the self-consistent renormalized model for itinerant magnetism, which provides good agreement with the measurements. At about 80 K, the Knight shifts and spin-lattice relaxation rates exhibit a crossover from Curie-Weiss magnetism to Korringa behavior. Comparing previously reported specific heat and transport results with our NMR results, we find that the Wilson ratio and Kadowaki-Woods relation are close to those observed for highly correlated electron compounds, despite the relatively small enhancement of  $\gamma$  and  $\chi$ . [S0163-1829(99)16835-8]

**I. INTRODUCTION**

$\text{Al}_3\text{V}$  is a well-ordered intermetallic trialuminide with a  $\text{DO}_{22}$  crystal structure.<sup>1</sup> A previous  $^{27}\text{Al}$  NMR study confirmed a low density of states at the Fermi level in this material.<sup>2</sup> Although the local electronic properties of  $\text{Al}_3\text{V}$  appear to be similar to other  $\text{DO}_{22}$  aluminides, a number of interesting features have been observed in this compound. For example, the reported resistivity measurements<sup>3</sup> showed a  $T^2$  dependence below 80 K with the coefficient  $A \approx 5.4 \times 10^{-4} \mu\Omega \text{ cm/K}^2$ . The  $T^2$  behavior suggests that electron-electron interactions dominate in this alloy. Moreover, its Kadowaki-Woods relation<sup>4</sup> [ $A/\gamma^2 \approx 1.6 \times 10^{-5} \mu\Omega \text{ cm} (\text{mole K/mJ})^2$  for the reported data<sup>3</sup>] between the coefficient  $A$  of the  $T^2$  resistivity term and the coefficient  $\gamma$  of the  $T$ -linear specific-heat term, is very close to that observed in systems showing strong many-body effects, such as the heavy fermion (HF) systems. However, the electronic heat-capacity coefficient ( $\gamma \approx 5.92 \text{ mJ/mole K}^2$ ),<sup>3</sup> is well below that of accepted HF materials.<sup>5</sup> Magnetic-susceptibility ( $\chi$ ) measurements<sup>6</sup> revealed Curie-Weiss (CW) behavior corresponding to a small moment, with a Weiss temperature  $\theta \approx -65 \text{ K}$  indicating antiferromagnetic spin interactions. There was no evidence for magnetic ordering, with  $\chi$  increasing with decreasing temperature down to 0.4 K.<sup>6</sup>

To investigate the magnetic and electronic behavior in  $\text{Al}_3\text{V}$ , we studied the temperature dependence of  $^{51}\text{V}$  and  $^{27}\text{Al}$  NMR Knight shifts as well as the spin-lattice relaxation rates in this compound. The Knight shift provides a local measurement of the susceptibility, which is less sensitive to the presence of impurities and other phases. The spin-lattice relaxation rate is sensitive to the excitation of quasiparticles around the Fermi level. Moreover, the NMR Korringa relation can yield information about electron-electron interactions. We show that the results are consistent with spin fluctuation behavior. An analysis using the self-consistent

renormalization (SCR) theory of spin fluctuations around an antiferromagnetic instability,<sup>7,8</sup> is found to give good agreement with the observations.

**II. EXPERIMENT**

The sample studied here was prepared by arc-melting in an Ar atmosphere. A portion of the resulting ingot was annealed in vacuum by placing it on a  $\text{Y}_2\text{O}_3$  plate at  $900^\circ\text{C}$  for 12 h. No change in NMR line shapes was detected in samples with or without annealing. An x-ray analysis was taken with  $\text{Cu } K\alpha$  radiation on the powder sample. The spectrum could be indexed according to the expected  $\text{DO}_{22}$  ( $\text{Al}_3\text{Ti}$  structure, a tetragonal lattice based on a fcc close-packed structure). The annealed ingot was ground to powder for NMR measurements, and placed in a plastic vial with granular quartz which showed no observable  $^{51}\text{V}$  and  $^{27}\text{Al}$  NMR signals.

$\text{Al}_3\text{V}$  contains two Al crystallographic sites, and one V site. Our group recently reported a study of the  $^{27}\text{Al}$  NMR in  $\text{Al}_3\text{V}$ , along with related aluminide intermetallics, at room temperature.<sup>2</sup> The central transition ( $m = -\frac{1}{2} \leftrightarrow +\frac{1}{2}$ ) powder line shape was found to reflect the combination of two Al crystallographic sites, according to the  $\text{DO}_{22}$  structure. We observed a larger anisotropic Knight shift at Al site I, which we also found in other trialuminides. The quadrupole frequencies,  $\nu_q$ , were determined to be 1.72 and 0.375 MHz for Al site I and site II, respectively. These values are also consistent with the recent results of another study.<sup>9</sup> The larger  $\nu_q$  and anisotropic Knight shift occurring at site I can be related to the directionality in binding which is believed to lead to brittleness in this alloy.

For  $^{51}\text{V}$ , the NMR line shape consists of a single central transition, along with six edge singularities corresponding to the first-order quadrupole transitions for  $I = \frac{7}{2}$   $^{51}\text{V}$ . The central transition line shape shows no structure because of the

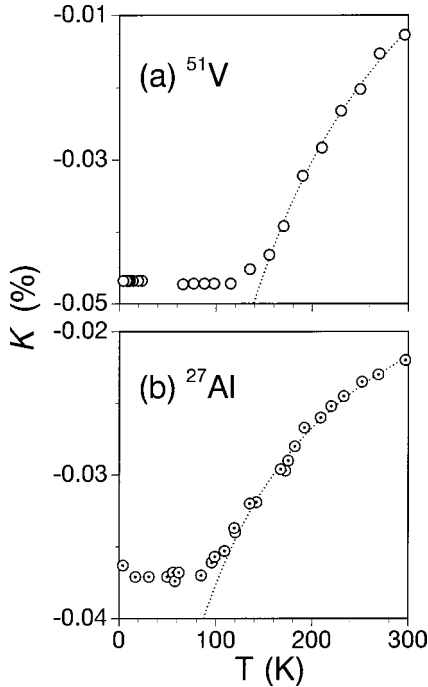


FIG. 1.  $T$  dependence of  $^{51}\text{V}$  and  $^{27}\text{Al}$  Knight shifts in  $\text{Al}_3\text{V}$ . Dotted curves are fits to the Curie-Weiss law.

single V site in  $\text{Al}_3\text{V}$ , and the absence of large anisotropic shifts. The measured  $\nu_q$  is about 0.39 MHz, determined directly from the peak edge of  $\pm\frac{1}{2} \leftrightarrow \pm\frac{3}{2}$  transitions.

Previous susceptibility measurements have been reported to satisfy a CW expression,  $\chi(T) = \chi_0 + \chi_d(T) = -5.7 + 1280/(T - \theta)$  in units  $10^{-5}$  emu/mole.<sup>6</sup>  $\chi_0$  is a  $T$ -independent term. The negative Weiss temperature  $\theta \approx -65$  K indicates antiferromagnetic spin interactions. The  $T$ -dependent susceptibility  $\chi_d$  originates from  $d$ -spin moments, and the Curie constant  $C = 1280 \times 10^{-5}$  emu K/mole can yield an effective moment  $P_{eff} = 0.32 \mu_B$  per vanadium.

### A. Knight shifts

The temperature dependences of  $^{51}\text{V}$  and  $^{27}\text{Al}$  Knight shifts, denoted as  $K_V$  and  $K_{Al}$ , respectively, are shown in Fig. 1.  $K_V$  reported here is the isotropic shift, corresponding to the peak position of the  $^{51}\text{V}$  central transition. For the case of  $^{27}\text{Al}$ , we report the shift of the peak of the central transition. Thus  $K_{Al}$  has contributions from both Al sites, and gives a relative measure of the isotropic Knight shifts. Little change was observed in  $^{27}\text{Al}$  line shape vs temperature, indicating that the two sites exhibit comparable temperature-dependent shifts. A detailed analysis of the  $^{27}\text{Al}$  isotropic and anisotropic shifts was reported earlier.<sup>2</sup>

Separating the components of  $K_V$ , we find that at high temperatures the spin component is proportional to the observed  $\chi(T)$ . The decrease in  $K_V$  with temperature corresponds to an increasing spin susceptibility because of the negative hyperfine field associated with the core-polarization mechanism, which typically dominates and has a negative sign in transition metals. The components of  $K_V$  are

$$K_V(T) = K_0 + K_d(T). \quad (1)$$

Here the  $d$ -spin shift  $K_d$  contains the temperature dependence, while  $K_0$  is a temperature-independent orbital term.  $K_0$  can be attributed to the Van Vleck susceptibility of  $d$  electrons, which should have little temperature dependence in this case.

A least-squares fit of the high-temperature  $K_V$  results to a CW  $\chi(T)$  expression is shown in Fig. 1(a). The relation between the Knight shift and spin susceptibility is,  $K_d = (2/\gamma_e \hbar) H_{hf}^d \chi_d$ , where  $H_{hf}^d$  is the  $d$ -spin core-polarization hyperfine coupling constant. In our fit we used the reported<sup>6</sup> CW behavior for  $\chi(T)$ , with  $P_{eff} = 0.32 \mu_B$  per vanadium atom and  $\theta = -65$  K, and allowed  $K_0$  and  $H_{hf}^d$  to vary. We obtained  $K_0 = 0.036\%$ , and  $H_{hf}^d = -83$  kG. The latter is quite consistent with the value ( $-86$  kG) calculated for V metal using local-spin-density-functional theory.<sup>10</sup> Thus the behavior of  $K_V$  shows that a uniform spin polarization at V sites is responsible for the observed CW behavior.

The high- $T$   $K_{Al}$  data can also be fit to a CW law, as shown by the dotted curve in Fig. 1(b). This shift (dominated by Al site II) originates from a transfer hyperfine interaction between the Al nucleus and V- $d$  electrons. In this case  $K_{Al} = (2/\gamma_e \hbar) H_{hf}^{tr} \chi_d Z$ , where  $H_{hf}^{tr}$  is the transfer hyperfine coupling constant and  $Z$  ( $=8$  for the  $\text{DO}_{22}$  structure) is the number of the nearest-neighbor V ions ‘‘seen’’ by Al site II. The coupling is negative for Al as for V, since a decrease in  $K$  is again seen to correspond to an increase in susceptibility. From our fit we obtain  $H_{hf}^{tr} = -2.4$  kG, which can be attributed to an intermixing of Al and V spin states. Since the Al  $s$ -contact hyperfine field is considerably larger than  $H_{hf}^{tr}$  ( $H_{hf}^s \approx 1.9$  MG),<sup>11</sup> the present result indicates very little spin content in Al  $s$  orbitals, relative to the observed spin susceptibility. Assuming the same to be true of Al  $p$  orbitals, and given the 3:1 Al:V atom ratio in this material, a virtual-bound-state picture (as originally described by Dunlop *et al.*<sup>3</sup>) in which vanadium moments are partially compensated for by conduction-band spins residing in the aluminum matrix, appears unlikely, since a relatively large Al spin-polarization would be expected. Indeed, in  $\text{Al}_3\text{V}$  as in the isostructural transition-metal trialuminides, the Al contribution to states at the Fermi level is relatively low,<sup>2</sup> so that a single-band picture based on  $d$  orbits is more appropriate.

While the high-temperature shifts are consistent with the observed bulk susceptibility,<sup>6</sup> below about 80 K  $K_V$  and  $K_{Al}$  become nearly independent of  $T$ , whereas  $\chi(T)$  continues to increase with decreasing temperature. This behavior could result from an orbital contribution to  $\chi(T)$ , giving an effective change in the hyperfine coupling behavior at low temperatures, as observed in heavy fermion materials.<sup>12</sup> However, hybridization would be expected to quench the orbital moment for this  $d$ -electron system. Another possibility is that the applied magnetic field in this experiment quenches the critical spin fluctuations. This will be examined in more detail below in Sec. III.

Removing the orbital contribution to the vanadium Knight shift, by subtracting  $K_0 = 0.036\%$  as obtained above, we find that the  $d$ -spin contribution to  $\chi(T)$  at low temperatures is  $K_d = -0.083\%$ . From  $K_d = (2/\gamma_e \hbar) H_{hf}^d \chi_d$ , the  $T$ -independent Pauli susceptibility is thus deduced to be  $5.6 \times 10^{-5}$  emu/mole, using the value  $H_{hf}^d = -83$  kG, calculated above.

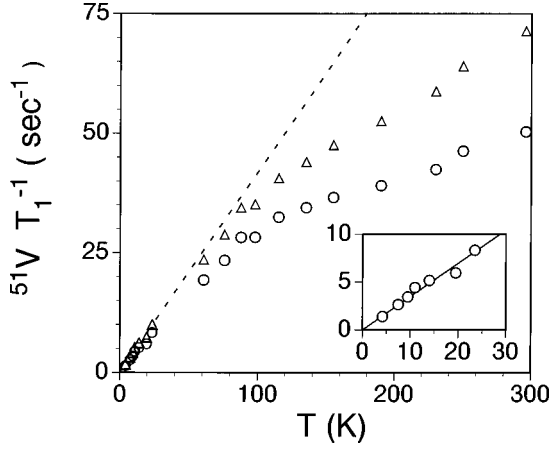


FIG. 2.  $T$  dependence of  $^{51}\text{V}$   $1/T_1$ 's. Open triangles and open circles represent the total relaxation rate and the  $d$ -spin component, separated as described in the text. The dashed lines indicate a Korringa relaxation mechanism below 80 K. The inset shows a linear plot of the low- $T$   $d$ -spin relaxation rates with  $(1/T_1 T)_d = 0.347 \text{ s}^{-1} \text{ K}^{-1}$ .

### B. Spin-lattice relaxation rates

The temperature dependences of the spin-lattice relaxation times ( $T_1$ 's) were measured using the pulse saturation recovery method in the  $T$  range of 4–300 K. We recorded the signal strength by integrating the spin-echo fast Fourier transform. The same technique has been applied to the semimetallic  $\text{Fe}_2\text{VAl}$  system.<sup>13</sup>  $^{51}\text{V}$   $T_1$ 's were measured at the central transition, while in order to separate the two sites we found the  $^{27}\text{Al}$   $T_1$  for each site by centering the resonance frequency at the  $m = -\frac{1}{2} \leftrightarrow -\frac{3}{2}$  quadrupole powder pattern edge, where the resonance is dominated by one site only. The  $^{51}\text{V}$  ( $I=7/2$ ) and  $^{27}\text{Al}$  ( $I=5/2$ )  $T_1$ 's were extracted by fitting to the appropriate theoretical multiexponential recovery curves,<sup>14</sup> for magnetic relaxation of the central transition and the satellites.

The  $^{51}\text{V}$   $T_1$  results are shown in Fig. 2.  $1/T_1$  is proportional to  $T$  below approximately 80 K, which is the Korringa behavior characteristic of nonmagnetic metals. This result matches the constant  $K_V$  observed in the same temperature range. Above 80 K,  $1/T_1$  falls below the Korringa relation, and is more closely proportional to  $\sqrt{T}$ , in the same temperature range in which  $K_V$  shows a Curie-Weiss behavior. In local-moment systems,  $T_1$  is characteristically independent of  $T$ , as observed in the Heusler alloys [e.g.,  $\text{In}_2\text{MnGa}$  (Ref. 15)].  $1/T_1$  proportional to  $\sqrt{T}$  is the behavior shown by Moriya<sup>7</sup> to correspond to itinerant-electron antiferromagnets above the Néel temperature.

As is the case for  $K_V$ , two terms dominate the  $^{51}\text{V}$   $T_1$ :  $(1/T_1) = (1/T_1)_{orb} + (1/T_1)_d$ . The first term is the orbital relaxation rate, while the second is due to  $d$ -spin interactions. Orbital relaxation in metals involves the overlap of orbitals of different symmetry at the Fermi level, giving generally  $(1/T_1)_{orb}$  proportional to  $T$ . To separate these terms, we used a two-parameter fit above 150 K, with  $(1/T_1)_{orb}$  linear in  $T$ , and  $(1/T_1)_d$  proportional to  $\sqrt{T}$ . The best-fit curve is plotted in Fig. 3, and thus we determined  $(1/T_1 T)_{orb} = 0.071 \text{ s}^{-1} \text{ K}^{-1}$ .

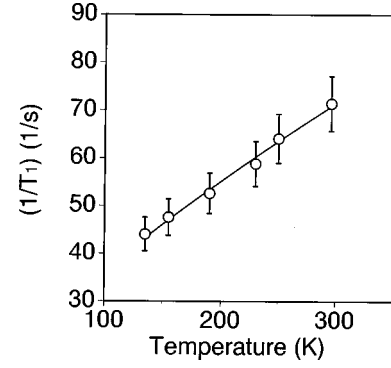


FIG. 3. High-temperature  $^{51}\text{V}$   $1/T_1$  vs  $T$ . Solid curve is a fit to  $T$ -linear orbital relaxation and  $\sqrt{T}$  spin term.

For  $D_{4h}$  symmetry, which is the V-site symmetry in  $\text{Al}_3\text{V}$ , a general expression for the orbital relaxation rate is<sup>16</sup>

$$(T_1)_{orb}^{-1} = A(H_{hf}^{orb})^2 \{ \sin^2 \theta (4n_{B_{1g}} n_{B_{2g}} + n_{E_g}^2) + [2 - \sin^2 \theta] n_{E_g} (3n_{A_{1g}} + n_{B_{1g}} + n_{B_{2g}}) \}, \quad (2)$$

where  $A = 2hk_B T \gamma_n^2$ ,  $H_{hf}^{orb}$  is the orbital hyperfine field per  $\mu_B$ , and  $\theta$  is the angle between the applied field and the  $c$  axis. The four terms  $n_{E_g}$ ,  $n_{A_{1g}}$ ,  $n_{B_{1g}}$ , and  $n_{B_{2g}}$  are Fermi-level densities of states corresponding to the irreducible representations of the  $D_{4h}$  group, defined so that the total density of states is,  $n_d(E_F) = n_{A_{1g}} + n_{B_{1g}} + n_{B_{2g}} + 2n_{E_g}$ . Of these four representations,  $E_g$  contains two  $d$  orbitals, while the others contain one orbital each.  $H_{hf}^{orb}$  can be estimated by using  $H_{hf}^{orb} = 2\mu_B \langle r^{-3} \rangle$ , where  $\langle r^{-3} \rangle$  is the average over the occupied  $d$  orbitals. Using  $\langle r^{-3} \rangle = 1.77 \times 10^{25} \text{ cm}^{-3}$ , calculated for V by Huzinaga *et al.*,<sup>17</sup> yields  $H_{hf}^{orb} = 330 \text{ kG}$ . For  $n_d(E_F)$  we use 0.9 (states/eV V atom), from Fig. 6 in Ref. 18, a recent first-principles electronic structure calculation [which can be compared to the measured<sup>3</sup>  $\gamma$ , which gives 2.5 (states/eV V atom)]. While the Fermi-surface orbital mixture is not known, the small observed  $(1/T_1 T)_{orb} = 0.071 \text{ s}^{-1} \text{ K}^{-1}$  is consistent with at most a few percent mixture of doubly degenerate  $E_g$ , using the parameters described above. We conclude that the dominant orbital at the Fermi level has a degeneracy equal to 1.

With  $(1/T_1 T)_{orb} = 0.071 \text{ s}^{-1} \text{ K}^{-1}$ , the  $d$ -spin relaxation rates can be isolated using  $(1/T_1)_d = (1/T_1) - (1/T_1)_{orb}$ , giving the results shown in Fig. 2. The figure inset is a linear plot of the low- $T$  relaxation rates with  $(1/T_1 T)_d = 0.347 \text{ s}^{-1} \text{ K}^{-1}$ , from a least-squares fit to a Korringa behavior. Above 80 K,  $(1/T_1)_d$  exhibits the same trend as identified above:  $(1/T_1)_d$  departs from a constant  $T_1 T$  and behaves as  $\sqrt{T}$  at high temperatures.

For  $^{27}\text{Al}$   $1/T_1$ 's, shown in Fig. 4, both Al sites display qualitatively the same  $T$  dependence as the  $^{51}\text{V}$   $1/T_1$ , indicating a related mechanism for the relaxation at both Al and V sites. This is due to the appearance of moments on Al through a transfer hyperfine interaction, which also strongly affects  $K_{Al}$ , as described above. At low temperatures we observed Korringa relaxation behavior for both site I and site II, with  $1/T_1 T = 4.7 \times 10^{-2}$  and  $2.7 \times 10^{-2} \text{ s}^{-1} \text{ K}^{-1}$ , respectively.

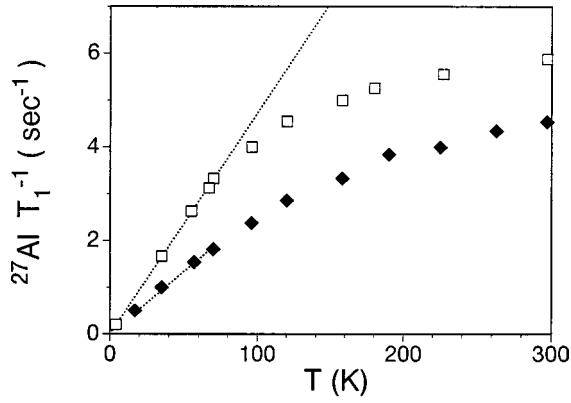


FIG. 4.  $T$  dependence of observed  $^{27}\text{Al}$   $1/T_1$ 's. Open squares and solid diamonds represent the  $1/T_1$  for Al sites I and II, respectively. Dotted lines indicate the Korringa relaxation below 80 K, with constant  $1/T_1 T = 4.7 \times 10^{-2}$  and  $2.7 \times 10^{-2} \text{ s}^{-1} \text{ K}^{-1}$ , respectively.

### III. DISCUSSION

The small-moment Curie-Weiss behavior and the absence of a magnetic transition observed in  $\text{Al}_3\text{V}$  point to spin fluctuations in an interacting  $d$ -band rather than localized moments. Furthermore, the  $\sqrt{T}$  behavior in  $^{51}\text{V}$   $T_1$  is characteristic of antiferromagnetic correlations in a spin-fluctuation model, as described above, also indicative of itinerant-electron character. Note that this picture differs from that of spin fluctuations within an  $s$ - $d$  model. Indeed, it is tempting to associate the crossover in  $K_V$  with  $T_{sf}$ , the Kondo spin-fluctuation temperature, since the behavior of  $K$  and  $T_1$  appears qualitatively much like the behavior of corresponding Kondo and heavy fermion systems.<sup>19</sup> However, as pointed out above, the Al matrix does not possess sufficient density of free electrons to support the formation of virtual bound states within such a model. While separate  $V$ -based  $d$  bands could produce this behavior if one of the bands is essentially localized, here we analyze the situation within a single-band model, showing good agreement with the observations.

Moriya<sup>7</sup> gives a momentum-space view of the fluctuation of localized and itinerant moments. In this picture, moments localized in space have a fluctuation spectrum almost independent of  $q$ . Hence the  $q$ -dependent susceptibility  $\chi_q$  is nearly constant, and the average amplitude of the local spin fluctuation,  $\langle S_L^2 \rangle$ , is fixed at  $S(S+1)$ . This situation leads to a  $T$ -independent  $T_1$  for local-moment systems. In contrast, itinerant-electron magnets are viewed as having an instability in the spin spectrum which is nearly localized in  $q$ . This instability occurs at  $q=0$  for cases of ferromagnetic order, while for antiferromagnetic (or nearly antiferromagnetic) metals,  $\chi_q$  peaks at a wave vector  $Q \neq 0$ . The latter situation is driven by band-structure features such as nesting which give peaks in the  $q$ -dependent susceptibility. An example of the nearly ferromagnetic case is  $\text{TiBe}_2$ ; its Knight shift exhibits Curie-Weiss behavior at high temperatures, but saturates at low temperatures with no magnetic order,<sup>20</sup> similar to the results observed in  $\text{Al}_3\text{V}$ .

The saturated low-temperature susceptibility in  $\text{TiBe}_2$  can be understood as a temperature-independent enhanced Pauli susceptibility. Significant progress in understanding the

higher-temperature magnetic behavior in such cases came from the SCR theory developed by Moriya<sup>3</sup> and others.<sup>21</sup> At high temperatures the Stoner enhancement is reduced due to repulsive mode-mode coupling,<sup>7</sup> and this can produce a temperature dependence identical to the Curie-Weiss behavior of localized moments. A crossover in measured susceptibility is due to the progressive reduction of the  $q=0$  mode due to these interactions. This model, valid at least in the weak-interaction limit,<sup>22</sup> provides a framework for the treatment of electron-electron interactions in metals. The SCR model has had considerable success, and recently additional interest has also been directed toward applications relating to high- $T_c$  superconductors.<sup>23</sup>

#### A. Korringa ratio

The Korringa ratio calculated from the low-temperature  $K$  and  $T_1$  can provide a measure of the fluctuation spectrum. For  $D_{4h}$  symmetry,  $(1/T_1)_d$  can be expressed as<sup>16</sup>

$$(T_1)_d^{-1} = A(H_{hf}^d)^2 [n_{A_{1g}}^2 + n_{B_{1g}}^2 + n_{B_{2g}}^2 + 2n_{E_g}^2], \quad (3)$$

with  $A = 2\hbar k_B T \gamma_n^2$  for noninteracting electrons. We demonstrated above that the  $E_g$  orbitals must play a minimal role. With little orbital mixing, the square bracket in Eq. (3) becomes simply  $n_d(E_F)^2$ , and  $(1/T_1)_d$  thus contains no orbital mixing factor (corresponding to the  $f$  factor for cubic metals<sup>24</sup>). For interacting electrons, Eq. (3) is modified as<sup>25</sup>

$$[(T_1)_d T]^{-1} = [(T_{1_0})_d T]^{-1} \left\langle \frac{1}{(1 - \alpha_q)^2} \right\rangle_{FS}, \quad (4)$$

where  $T_{1_0}$  expresses the noninteracting case, and  $\alpha_q = \alpha_0 \chi_0(q) / \chi_0(0)$  is the  $q$ -dependent susceptibility enhancement, with  $\alpha_0 = 1 - \chi_0(0) / \chi(0)$  representing the  $q=0$  value. The symbol  $\langle \rangle_{FS}$  means the average over  $q$  space on the Fermi surface. The Korringa ratio is

$$K^2 T_1 T / S = [K(\alpha)]^{-1}, \quad (5)$$

with  $S = \hbar / 4\pi k_B (\gamma_e / \gamma_n)^2$ , and where

$$K(\alpha) = \left\langle \frac{(1 - \alpha_0)^2}{(1 - \alpha_q)^2} \right\rangle_{FS}. \quad (6)$$

Using the low- $T$  values  $(1/T_1 T)_d = 0.347 \text{ s}^{-1} \text{ K}^{-1}$ , and  $K_d = -0.083\%$ , we obtain  $K(\alpha) \approx 1.9$  in  $\text{Al}_3\text{V}$  (a Korringa ratio of 0.5). For comparison,  $K(\alpha)$  was found to be 0.032 in  $\text{TiBe}_2$ ,<sup>20</sup> and 0.42 in  $\text{CoTi}$  (Ref. 26); small values of  $K(\alpha)$  can be viewed as indicating a narrow peak of enhanced  $\chi_q$ , localized at  $q=0$ .  $K(\alpha) > 1$ , as observed in  $\text{Al}_3\text{V}$ , can be produced by an enhanced susceptibility which peaks away from  $q=0$ , so that the denominator in Eq. (6) outweighs the numerator. This would indicate a tendency toward antiferromagnetic ordering (at  $q \neq 0$ ). While the case  $K(\alpha) > 1$  is uncommon (usually the Knight shift is more strongly exchange enhanced than  $1/T_1$ ), similar behavior has been observed in the recently proposed  $d$ -electron heavy fermion system  $\text{LiV}_2\text{O}_4$  for which  $K(\alpha) \approx 1.4$ .<sup>27</sup> In that case, the anomalies in  $^7\text{Li}$  NMR were analyzed in terms of spin fluc-



tuations near a magnetic instability within the SCR theory (although in a nearly-ferromagnetic model).<sup>28</sup>

### B. SCR model parameters

In the SCR model, a set of parameters ( $y_0$ ,  $y_1$ ,  $T_0$ , and  $T_A$ ) have been introduced as a relative measure of the magnetic instability in  $q$  space.<sup>8,29</sup> These parameters, based on a spherical Brillouin-zone approximation, provide a means to assess quantitatively the spin-fluctuation behavior.  $T_0$  and  $T_A$  give (in temperature units) the width of the susceptibility peak, in energy and in  $q$  space, respectively, while  $y_0$  and  $y_1$  are dimensionless parameters measuring the nearness to a magnetic transition.  $T_0$ ,  $T_A$ , and  $y_0$  can be related to the  $T=0$  behavior only, while  $y_1$  relates to the temperature dependence. Recently, number of different materials has been analyzed this way.<sup>8,28,30</sup>

The parameter  $T_A$  can be determined from the static uniform susceptibility<sup>8</sup>

$$\chi = \frac{(g\mu_B)^2}{2k_B T_A (1+y)\alpha_Q}, \quad (7)$$

where  $y = (g\mu_B)^2 / 2k_B T_A \alpha_Q \chi_Q$  is (for the nearly antiferromagnetic case) the reduced inverse staggered susceptibility.  $Q$  refers to the instability wave vector, and  $\alpha_Q \approx 1$  if there is significant exchange enhancement. The zero-temperature value for  $y$  is defined as  $y_0$ . Since  $y_0 \ll 1$  for enhanced materials, this term can be neglected in Eq. (7). We use the low-temperature constant  $K_d$  as a measure of the spin susceptibility, with  $K_d = H_{hf}^d \chi / \mu_B$ . This gave  $\chi = 5.6 \times 10^{-5}$  emu/mole, as described above, and thus the value  $T_A \approx 13300$  K is obtained.

A measure of  $y_0$  and  $T_0$  is obtained from the  $T_1$ , generally given by<sup>25</sup>

$$\frac{1}{T_1} = \frac{\hbar \gamma_n^2 T}{N_0} \sum_q \frac{|H_q|^2 \text{Im} \chi^{-+}(q, \omega_0)}{\omega_0}, \quad (8)$$

where  $H_q$  is the  $q$  Fourier-component of the hyperfine coupling constant, and  $\omega_0$  is the NMR frequency. In the SCR model the dynamical susceptibility for antiferromagnets is given as<sup>8</sup>

$$\chi(Q+q, \omega) = \frac{\pi T_0}{\alpha_Q T_A} \frac{(g\mu_B)^2}{2\pi T_0 (y+x^2) - i\omega}, \quad (9)$$

where  $x = q/q_B$ , with  $q$  representing the relative displacement from the instability wave vector  $Q$ , and with  $q_B$  the Brillouin-zone wave vector (in a spherically symmetric approximation). Inserting Eq. (9) into Eq. (8), and neglecting the  $q$  dependence of  $H_q$ , integration yields the low- $T$  relaxation rate<sup>8</sup>

$$\frac{1}{T_1} = \frac{3\hbar \gamma_n^2 (H_{hf}^d)^2 T}{8k_B T_A T_0 \sqrt{y_0}}. \quad (10)$$

To determine the unknown parameters  $y_0$  and  $T_0$  contained in Eq. (10), we can further use the specific heat, reported in Ref. 3. The  $T$ -linear coefficient of the specific heat (per atom) due to spin fluctuations at low temperatures ( $T \ll T_0$ ) is given as<sup>29</sup>

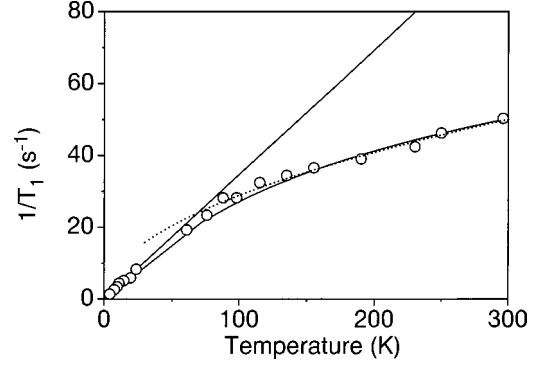


FIG. 5. Temperature dependence of  $^{51}\text{V}$   $(1/T_1)_d$  (circles), compared with the SCR model for spin fluctuations near an antiferromagnetic instability. The lower curve is calculated using the SCR parameters described in the text. The solid line is the corresponding Korringa behavior [ $(1/T_1 T)_d = 0.347 \text{ s}^{-1} \text{ K}^{-1}$ ], while the dotted curve is a  $\sqrt{T}$  dependence from the high-temperature fit.

$$\gamma = -\frac{3k_B}{4T_0} \ln(y_0). \quad (11)$$

We substitute  $T_A \approx 13300$  K in Eq. (10), and combine with Eq. (11), using  $\gamma = 5.92 \text{ mJ/mole K}^2$ ,<sup>3</sup>  $H_{hf}^d = -83 \text{ kG}$ ,  $\gamma_n/2\pi = 1.1193 \text{ kHz/G}$ , and the low-temperature  $^{51}\text{V}$   $(1/T_1 T)_d = 0.347 \text{ s}^{-1} \text{ K}^{-1}$ . This yields  $T_0 = 7520$  K and  $y_0 = 0.00079$ .

The parameter  $y_0$  is the reciprocal of the  $T=0$  exchange enhancement, measured at the instability peak. Thus a system with infinite enhancement, unstable to magnetic order, would have  $y_0 = 0$ . A small positive value of  $y_0$ , as found here, implies a near instability, and the value we report implies that the enhancement is approximately  $10^2$  at its peak.

The additional parameter  $y_1$  determines the temperature dependence of  $y$ , and therefore  $\chi$ , in the SCR model. For an antiferromagnetic instability this is<sup>8</sup>

$$y = y_0 + \frac{3}{2} y_1 \int_0^1 dx x^2 \left[ \ln u - \frac{1}{2u} - \psi(u) \right], \quad (12)$$

with  $u = T_0(y+x^2)/T$ , and where  $\psi(u)$  is the digamma function. The temperature dependence of  $T_1$  follows by replacing  $y_0$  with  $y$  in Eq. (10). From numerical integration of Eq. (12) we find that  $y_1 = 1.4$  gives very good agreement with the measured  $(1/T_1)_d$ , as shown in Fig. 5. Also shown in Fig. 5 are curves corresponding to the low-temperature Korringa behavior with  $(1/T_1 T)_d = 0.347 \text{ s}^{-1} \text{ K}^{-1}$ , and the  $\sqrt{T}$  dependence that characterizes the high-temperature portion of the data. The  $\sqrt{T}$  curve uses the parameter extracted from the least-squares fit described above, from the determination of  $(1/T_1)_{orb}$ . Thus we see that  $(1/T_1)_d$  goes smoothly from a Korringa to a  $\sqrt{T}$  behavior, following the detailed theory of Eq. (12) quite well.

The SCR parameters determined here are typical of those found for  $d$ -electron metals close to an instability.<sup>8</sup> For instance,  $y_1 = 0.5$  was found for the antiferromagnet  $\text{V}_2\text{O}_3$ , with  $T_0 = 390$  K and  $T_A = 4800$  K, while for the weak ferromagnet  $\text{Ni}_3\text{Al}$ ,  $T_0 = 3600$  K and  $T_A = 31000$  K. Heavy fermion  $f$ -electron materials have also been treated within the SCR model, with significantly smaller values of  $T_0$  and

$T_A$ ,<sup>31,30</sup> reflecting the smaller temperature scale and more enhanced susceptibility in those materials.

Thus the SCR model provides a consistent explanation of the  $\text{Al}_3\text{V}$  NMR and specific heat: electron-electron interactions lead to a large enhancement in  $\chi_q$ , and a smaller enhancement of  $\gamma$  (the values quoted above<sup>3,18</sup> indicate a  $\gamma$  enhancement of 2.8, comparable to what is found in paramagnon systems). That the  $\chi_q$  enhancement occurs at an antiferromagnetic wave vector was deduced from the  $\sqrt{T}$  dependence of  $(1/T_1)_d$ , and from the magnitude of the low-temperature Korringa ratio. However, the Curie-Weiss behavior of  $\chi$  in the SCR model requires the enhancement to encompass  $q=0$  (since the  $q=0$  term corresponds to the static susceptibility).<sup>7</sup> One possibility is that  $\chi_q$  is more complicated than given by this simple model, with peaks both at  $q=0$  and at an antiferromagnetic wave vector, which could result from the details of the band structure. A  $q=0$  component to the fluctuation spectrum will also lead to suppression of the  $q=0$  part of the fluctuation spectrum by the magnetic field. Indeed, magnetic fields are known to affect weakly ferromagnetic materials<sup>8,32</sup> (though not antiferromagnetic). This can also explain the departure of  $K_V$  from the bulk susceptibility. In this case, the NMR parameters will somewhat underestimate the susceptibility enhancement, and  $y_0$  should be smaller (though still nonzero). However, a multi-peaked structure for  $\chi_q$  would then be required to explain the NMR Korringa ratio. A similar situation may be responsible for the Korringa ratio in  $\text{LiV}_2\text{O}_4$ .<sup>27,28</sup>

### C. Other comparisons

For comparison with other weakly magnetic materials, it is instructive to examine the Wilson ratio  $R_W \equiv (\pi k_B)^2 \chi / 3 \mu_B^2 \gamma$ . Using the low-temperature spin susceptibility deduced from  $K_V$ ,  $\chi = 5.6 \times 10^{-5}$  emu/mole as given above, and  $\gamma = 5.92$  mJ/mole  $\text{K}^2$ ,<sup>3</sup>  $R_W = 0.7$  is obtained. (Using the  $T=0$  bulk  $\chi$  value gives  $R_W = 1.4$ .) We have not corrected for electron-phonon coupling, but  $\lambda$  is likely small in this nonsuperconducting material, so that the correction to  $\gamma$  should not be large. Spin-fluctuation enhancement is stronger for  $\chi$  than for  $\gamma$  in ordinary metals, giving a value of  $R_W$  considerably larger than 1.  $R_W \approx 1$  is typically observed in heavy fermion materials, and this value is often taken as an indication of exotic behavior.<sup>33,34</sup> For fluctuations which peak at  $Q \neq 0$ , however, the susceptibility enhancement will

not be as large, as described above (this was responsible for the small Korringa ratio). Thus the Wilson ratio can be understood in terms of  $q$ -dependent spin fluctuations.

Another measure of this behavior is the Kadawaki-Woods relation,<sup>4</sup> which relates  $A$  (the coefficient of the  $T^2$  resistivity term) to  $\gamma$ . The resistivity of  $\text{Al}_3\text{V}$  was found to follow a  $T^2$  law quite accurately,<sup>3</sup> indicative of electron-electron interactions. Taking values from Ref. 3, one finds for  $\text{Al}_3\text{V}$  that  $A/\gamma^2 = 1.6 \times 10^{-5} \mu\Omega \text{ cm}(\text{mole K/mJ})^2$ . Like  $R_W$ , this ratio is often used as a measure of exotic behavior,<sup>33,34</sup> and the value found here is also very close to the value originally identified as characteristic of heavy fermion materials.  $3d$  transition metals such as Pd exhibit  $A/\gamma^2$  an order of magnitude smaller than the heavy fermion value, but a number of intermetallics such as the A15 materials<sup>35</sup> have shown  $A/\gamma^2$  falling on the universal curve. It has been suggested<sup>35</sup> that this indicates similar many-body effects operating in these  $3d$  intermetallics and in the heavy fermion materials. It is interesting that in  $\text{Al}_3\text{V}$  we have an intermetallic with a small enhancement of  $A$  and  $\gamma$ , whose ratio still falls on the same curve. In fact, of the many materials found to fall on this curve,<sup>4,34,35</sup>  $\text{Al}_3\text{V}$  has the smallest values of  $A$  and  $\gamma$  of which we are aware.

## IV. CONCLUSIONS

In conclusion, we have studied the magnetic behavior of  $\text{Al}_3\text{V}$  using NMR as a probe. We identified the weak Curie-Weiss behavior as due to spin magnetism based in vanadium  $d$  orbitals. Analysis showed the behavior to be consistent with spin fluctuations related to incipient antiferromagnetic order, and the SCR model provided good agreement with both the NMR results and previously reported specific-heat data. We propose a complex wave-vector dependence of  $\chi_q$  in order to account for the low-temperature NMR and susceptibility results. In addition, we have shown that the Wilson ratio and  $A/\gamma^2$  are in the range of strongly interacting electron systems, even though the enhancement of  $\gamma$  is relatively small.

## ACKNOWLEDGMENTS

We are grateful to D. G. Naugle and K. D. D. Rathnayaka for help with sample preparation. This work was supported by Texas A&M University.

\*Electronic address: c019877@unix.tamu.edu

†Electronic address: jhross@tamu.edu

<sup>1</sup>W. B. Pearson, *A Handbook of Lattice Spacings and Structures of Materials and Alloys* (Pergamon, Oxford, 1967); *Structure Reports* (International Union of Crystallography, Utrecht, 1967), Vol. 32, Pt. A, p. 14.

<sup>2</sup>Chin-Shan Lue, Suchitra Chepin, James Chepin, and Joseph H. Ross, Jr., *Phys. Rev. B* **57**, 7010 (1998).

<sup>3</sup>J. B. Dunlop, G. Gruner, and A. D. Caplin, *J. Phys. F* **4**, 2203 (1974).

<sup>4</sup>K. Kadawaki and S. B. Woods, *Solid State Commun.* **58**, 507 (1986).

<sup>5</sup>Z. Fisk, D. W. Hess, C. J. Pethick, D. Pines, J. L. Smith, J. D. Thompson, and J. O. Willis, *Science* **239**, 33 (1988).

<sup>6</sup>L. Creveling, Jr. and H. L. Luo, *Phys. Lett.* **28A**, 772 (1969).

<sup>7</sup>Toru Moriya, *Spin Fluctuations in Itinerant Electron Magnetism* (Springer-Verlag, Berlin, 1985).

<sup>8</sup>A. Ishigaki and T. Moriya, *J. Phys. Soc. Jpn.* **65**, 3402 (1996).

<sup>9</sup>T. J. Bastow, C. T. Forwood, M. A. Gibson, and M. E. Smith, *Phys. Rev. B* **58**, 2988 (1998).

<sup>10</sup>H. Ebert, H. Winter, and J. Voitländer, *J. Phys. F* **16**, 1133 (1986).

<sup>11</sup>*Metallic Shifts in NMR*, edited by G. C. Carter, L. H. Bennett, and D. J. Kahan (Pergamon, Oxford, 1977).

<sup>12</sup>D. E. MacLaughlin, F. R. de Boer, J. Bijvoet, P. F. de Châtel, and W. C. M. Mattens, *J. Appl. Phys.* **50**, 2094 (1979).

<sup>13</sup>Chin-Shan Lue and Joseph H. Ross, Jr., *Phys. Rev. B* **58**, 9763 (1998).

- <sup>14</sup>A. Narath, Phys. Rev. **162**, 320 (1967).
- <sup>15</sup>K. Yoshimura, M. Yamada, M. Mekata, T. Shimizu, and H. Yasuoka, J. Phys. Soc. Jpn. **57**, 409 (1988).
- <sup>16</sup>B. Nowak and O. J. Zogał, Solid State Nucl. Magn. Reson. **1**, 251 (1992).
- <sup>17</sup>S. Huzinaga, J. Andzelm, M. Kłobukowski, E. Radzio-Andzelm, Y. Sakai, and H. Tatewaki, *Gaussian Basis Sets for Molecular Calculations* (Elsevier, Amsterdam, 1984).
- <sup>18</sup>M. Weinert and R. E. Watson, Phys. Rev. B **58**, 9732 (1998).
- <sup>19</sup>K. Levin, J. H. Kim, J. P. Lu, and Q. Si, Physica C **175**, 449 (1991).
- <sup>20</sup>S. Takagi, H. Yasuoka, J. L. Smith, and C. Y. Huang, J. Phys. Soc. Jpn. **53**, 3210 (1984).
- <sup>21</sup>K. K. Murata and S. Doniach, Phys. Rev. Lett. **29**, 285 (1974).
- <sup>22</sup>K. Okumura, Phys. Rev. B **52**, 13 358 (1995).
- <sup>23</sup>M. J. Lercher and J. M. Wheatley, J. Magn. Magn. Mater. **185**, 384 (1998).
- <sup>24</sup>Y. Yafet and V. Jaccarino, Phys. Rev. **133**, A1630 (1964).
- <sup>25</sup>T. Moriya, J. Phys. Soc. Jpn. **18**, 516 (1963).
- <sup>26</sup>A. Shinogi, K. Endo, Y. Kitaoka, and H. Yasuoka, J. Phys. Soc. Jpn. **53**, 4117 (1984).
- <sup>27</sup>S. Kondo, D. C. Johnson, C. A. Swenson, F. Borsa, A. V. Mahajan, L. L. Miller, T. Gu, A. I. Goldman, M. B. Maple, D. A. Gajewski, E. J. Freeman, N. R. Dilley, R. P. Dickey, J. Merrin, K. Kojima, G. M. Luke, Y. J. Uemura, O. Chmaissem, and J. D. Jorgensen, Phys. Rev. Lett. **78**, 3729 (1997).
- <sup>28</sup>N. Fujiwara, H. Yasuoka, and Y. Ueda, Phys. Rev. B **57**, 3539 (1998).
- <sup>29</sup>A. Ishigaki and T. Moriya, J. Phys. Soc. Jpn. **65**, 376 (1996).
- <sup>30</sup>S. Kambe, J. Flouquet, and T. E. Hargreaves, J. Low Temp. Phys. **108**, 383 (1997).
- <sup>31</sup>T. Moriya and T. Takimoto, J. Phys. Soc. Jpn. **64**, 960 (1995).
- <sup>32</sup>K. Ikeda, M. Yoshizawa, S. K. Dhar, and K. A. Gschneidner, Jr., J. Magn. Magn. Mater. **100**, 292 (1991).
- <sup>33</sup>A. C. Hewson, *The Kondo Problem to Heavy Fermions* (Cambridge University Press, Cambridge, 1993).
- <sup>34</sup>B. Brandow, Phys. Rep. **296**, 1 (1998).
- <sup>35</sup>K. Miyake, T. Matsuura, and C. N. Varma, Solid State Commun. **71**, 1149 (1989).